ARTICLES

An Optical and Theoretical Investigation of the Ultrafast Dynamics of a Bisthienylethene-Based Photochromic Switch

P. R. Hania,[†] R. Telesca,[‡] L. N. Lucas,[§] A. Pugzlys,[†] J. van Esch,[§] B. L. Feringa,[§] J. G. Snijders,[‡] and K. Duppen*,[†]

Ultrafast Laser and Spectroscopy Laboratory, Theoretical Chemistry, Organic Chemistry and Catalysis, Materials Science Center, Rijksuniversiteit Groningen, Nijenborgh 4, 9747 AG Groningen, The Netherlands

Received: April 4, 2002; In Final Form: July 5, 2002

The switching behavior of 1,2-bis(5-phenyl-2-methylthien-3-yl)cyclopentene is studied by means of polarization selective nonlinear optical spectroscopy and time-dependent density functional theory. The combined information from the observed population and orientational dynamics together with the results of theoretical calculations show that on a subpicosecond time scale rapid mixing and relaxation of electronic states occur, before switching takes place. Such preswitching dynamics was not studied in detail in these systems before. Then, the switching process itself occurs by the formation of a C−C bond in the central cyclopentene ring with a time constant of 4.2 ps. Driven by the ring closure, the side groups of the switch molecules rotate to a nearly coplanar conformation with a time constant of about 8 ps. The switching process is completed by relaxation of the vibrationally hot ground state of the closed form of the molecule to thermal equilibrium.

I. Introduction

In recent years, there has been increasing interest in the synthesis, investigation, and application of organic photochromic materials as a possible basis for optoelectronic and photooptical devices. Diarylethenes with heterocyclic aryl groups belong to a new class of thermally irreversible photochromic switches. Besides low fatigue and high thermal stability, diarylethenes and, in particular, bisthienylethene (BTE)-based compounds feature remarkable switching sensitivity (high quantum yield) and rapid response.[1,2]

Photochromism is defined as a reversible photoinduced chemical reaction during which optical, dielectric, and conformational properties of molecules change. In Figure 1 the chemical structures of 1,2-bis(5-phenyl-2-methylthien-3-yl)-cyclopentene (B-DTCP) in the open- (**1A**) and closed-ring (**1B**) configurations are presented. The ground-state interconversion between the isomers is prohibited but upon UV irradiation **1A** converts to **1B.** As a consequence of the near-coplanar geometry of the thiophene moieties of **1B**, the π-conjugation spreads throughout the molecule, resulting in the appearance of a new red-shifted absorption band. Upon visible irradiation this conjugation is broken again by opening the ring to yield the initial open form **1A** again. The steady-state absorption spectra of **1A** and **1B** are presented in Figure 2 (for more details see section III).

In the past decade many experimental investigations on the switching dynamics of various photochromic compounds were performed including both ring-closure[3−6] and ring-opening[7−9] reactions. The time constants reported in the literature for ring-opening reactions vary from 2.2 ps[7] and <10 ps[3] to 325 ps,[8] whereas ring-closure times in most cases are substantially shorter and much less spread. For instance, pump−probe experiments

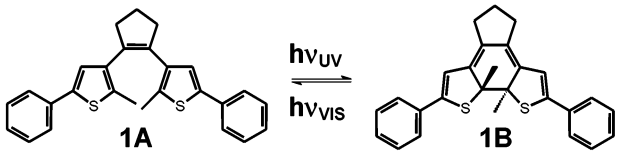

Figure 1. Chemical structure of the B-DTCP molecule in the open (1A) and closed (1B) forms. Interconversion is possible by irradiation with UV (1A → 1B) and with visible (1B → 1A) light.

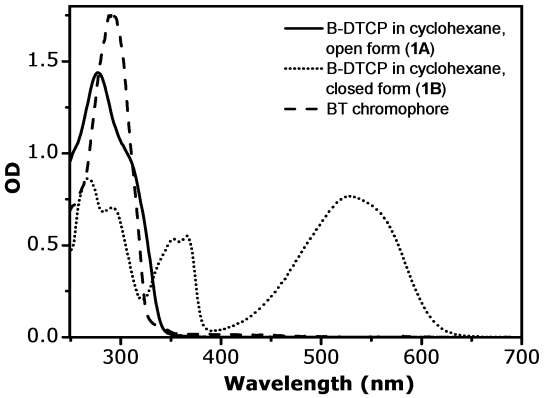

Figure 2. Steady-state absorption spectra of B-DTCP in the open form (solid line), B-DTCP in the closed form (dotted line), and BT-chromophore (dashed line) that constitutes the side groups of B-DTCP. The solvent is cyclohexane.

* To whom correspondence should be addressed. Tel: +31.50.3634560. Fax: +31.50.3634441. E-mail: K.Duppen@chem.rug.nl.
[†] Ultrafast Laser and Spectroscopy Laboratory.
[‡] Theoretical Chemistry.
[§] Organic Chemistry and Catalysis.

10.1021/jp020903+ CCC: $22.00
Published on Web 08/27/2002

on several dithienylperfluorocyclopentene switches have revealed ring-closure time constants from 1 to 3 ps.[4−6,10] The different switching time constants presumably originate from differences in the chemical structure of the investigated compounds.

Woodward−Hoffmann rules for electrocyclic reactions[11] predict in the case of 6π-electron ring-closure a concerted one-step mechanism through a conrotatory path in the excited state.[12] Indeed, no intermediates in the pathway of the ring-closure reaction were found by Ern et al.[10] in the case of 1,2-bis(5-formyl-2-methylthien-3-yl)perfluorocyclopentene, by Ohtaka et al.[5] in the case of diarylethene derivatives with terthiophene, and by Owrutsky et al.[6] in the case of 1,2-bis(5-pyridyl-2-methylthien-3-yl)perfluorocyclopentene. In contrast, for a diarylethene structure with thiophene oligomers as side groups, Tamai et al.[4] reported the rapid (∼100 fs) formation of an intermediate state, followed by ring closure with a time constant of about 1.1 ps. In that study the nature of the intermediate precursor states was not discussed. Electronic-conformational relaxation to a precursor state on a time scale of about 0.9 ps, followed by ring closure with a time constant of about 10 ps, was also reported by Ern et al.[13] in the case of 1,2-bis(5-anthryl-2-methylthien-3-yl)perfluorocyclopentene. Recently the existence of a precursor to the ring closure that is formed within less than 1 ps was reported by Bens et al.[14] for di-bpe dithienylethene.

All the measurements reported so far were performed with a time resolution of a few hundred of femtoseconds. In this paper we present results of spectroscopic studies on the switching behavior of B-DTCP with a time resolution below 100 fs. In this way the presence or absence of precursor states to the ring-closure reaction itself can be unequivocally established. To our knowledge, the work presented here is the first study of dithienylcyclopentene switches possessing nonfluorinated cyclopentene moieties. Because the ring closure by definition is related to conformational changes in the molecule, a second goal of our studies is to trace the orientational dynamics in the switch molecule during the ring-closure reaction. This should provide important information on the mechanism of the switching process. The nature of the electronic states, involved in the ring-closure reaction, is established by comparing the experimental results to electronic structure calculations, using density functional theory.

The paper is organized as follows: in section II the experimental setup and main concepts of the experiments are described. The results of femtosecond pump−probe and transient anisotropy experiments are presented in section III. These results are discussed and related to a theoretical analysis of the electronic structure in section IV. The conclusions are summarized in section V.

II. Experimental Section

Compound **1A** (see Figure 1) was synthesized starting from 1,2-bis(5′-chloro-2′-methylthien-3′-yl)cyclopentene[15] via a Suzuki reaction according to a slightly modified procedure described by Lehn et al.[16] For the optical experiments, **1A** was dissolved in cyclohexane (p.a., Merck) at a concentration of 0.7 mM. The solution was pumped at a speed of about 3 mL/s to ensure that fresh sample was available for every single measurement. The optical density of the sample did not exceed 0.3, ensuring homogeneous excitation. The experiments were performed at room temperature (T = 294 K).

Femtosecond polarization selective frequency resolved pump−probe experiments were performed by using a 1 kHz Ti:sapphire laser system (Hurricane, Spectra Physics) and optical parametric amplifiers (OPA). The laser system produces 120-fs, 800-μJ pulses at 1 kHz, centered at 800 nm. About 300 μJ of that energy is used to pump a travelling wave optical parametric amplifier of superfluorescence (TOPAS, Light Conversion LTD), which is employed to generate the pump pulses. The sample is excited with 70-nJ pulses centered at 310 nm (fourth harmonics of the signal wave of the TOPAS at 1240 nm). Before the generation of 310 nm light, the second harmonics of the output of the TOPAS (620 nm) is compressed in a double-pass compressor based on two BK7 prisms. In addition to the pulse shortening, the compressor allows the spatial separation of different spectral components of the parametric light (signal and idler beams). The polarization of the pump beam is changed by using a $\lambda/2$ plate.

The probe pulses are generated in a home-built noncollinearly pumped optical parametric amplifier (NOPA[17]). Briefly, the 1-mm type I BBO crystal of the NOPA is pumped by pulses with an energy of about 10 μJ centered at 400 nm. The pulses are tilted by passing them through a 45° fused silica prism and subsequently focused onto the crystal by a spherical mirror of r = 40 cm. A white light continuum generated in a 2 mm sapphire plate is used as a seed for the NOPA. Before amplification, the white light is precompressed in a compressor, based on a 1200 mm^{-1} grating and a curved mirror (Light Conversion LTD) designed to compensate for the enhanced angular dispersion of the grating at the red side of the spectrum. A mask placed in the compressor allows spectral selection and shaping of the probe pulse. The NOPA produces pulses with an energy of about 0.5 μJ that are tunable in the spectral region 450−900 nm. By generating second harmonics in a 150-μm BBO crystal, the tunability can be extended to the UV spectral region (230−450 nm).

The time resolution of the experiments is probe wavelength dependent. In the spectral region 460−750 nm the duration of the probe pulses is about 30 fs and the time resolution is mainly determined by the duration of the pump pulse. The cross-correlation function of the pump pulse centered at 310 nm and the probe pulse centered at 600 nm, as measured by monitoring two-color two-photon absorption in a 100-μm glass plate,[18] has a width of about 90 fs fwhm. The probe pulses, produced by generating second harmonics from the NOPA output, are slightly stretched because of the spectral filtering in the BBO doubling crystal. For the wavelength range of 380−450 nm (second harmonics from 760 to 900 nm light) the time resolution is degraded to about 110 fs because of strong spectral phase distortion of the white light around the carrier wavelength 800 nm.

The transients of the photoinduced absorption are measured in a standard pump−probe geometry. The probe pulse before the sample is split into two to serve as both probe and reference. The probe pulse is delayed with respect to the pump pulse by using a computer-controlled delay stage, whereas the reference pulse is set to reach the sample before the pump and probe pulses arrive. The pump, probe, and reference pulses after attenuation are focused by a spherical mirror of r = 25 cm into a 200-μm flow cell containing the sample. They are all monitored by silicon photodiodes connected to a sample-and-hold device. During the measurements, every second pump pulse is blocked using a chopper that is synchronized with the laser. Optical density changes (ΔOD) in absolute units are calculated for every single pair of probe pulses and then averaged over 50 measurements. To monitor zero delay between pump and probe

pulses, a cross-correlation function of pump and probe pulses is measured for every probe wavelength.

In a separate experiment the dynamics of the whole pump−probe spectrum is recorded by using white light probe pulses, generated in a standing 1 cm doubly distilled water cell, and monitored via a polychromator in a double-array OMA system (Princeton Instruments). The pump beam is opened/closed every 2 s to obtain difference spectra (ΔOD). Because these white light pulses have a large temporal dispersion, which is hard to correct accurately, the early time ΔOD spectra reported in the next section are constructed from single color pump−probe measurements as described above. The construction is possible because the ΔOD values are measured in absolute units and because the zero delay position between the pump and probe pulses is known.

III. Results

3.1. Photoconversion Pathways. The steady-state absorption spectrum of the open form of B-DTCP (**1A**), dissolved in cyclohexane, is presented in Figure 2. In addition, the steady-state absorption spectrum of the 2-phenyl-5-methylthiophene (BT) chromophore (0.1 mM solution in a 1 mm quartz cell) is given. The fact that there is only a small difference between the shapes of the steady-state absorption spectra of B-DTCP and the BT chromophore indicates that the electronic interaction between the two BT groups in the **1A** molecule is rather weak.

Upon photoexcitation by UV light (extinction coefficient $\epsilon_{\mathbf{1A},310} = (21.2 \pm 0.3) \times 10^3$ L mol^{-1} cm^{-1}), the open form **1A** is converted into the closed form **1B** via a cyclization (ring-closure) reaction. This results in a spread of π-conjugation throughout the molecule and, consequently, in the appearance of a new red-shifted absorption band. Because of nonzero absorption of both the open and closed forms in the UV spectral region, simultaneously ring closure and ring opening take place upon UV irradiation. This leads to an equilibrium situation determined by the relative quantum yields of the processes and results in an absorption spectrum that is determined by both the open-ring and closed-ring conformers. The ratio between the number of B-DTCP molecules in open-ring and closed-ring forms can be determined by proton NMR spectroscopy. Then the steady-state absorption spectrum of the closed form (Figure 2) is obtained by subtracting the open-form absorption spectrum from the absorption spectrum of the mixture of closed-ring and open-ring molecules.

It is important to realize that the analysis of the ring-closure reaction is complicated because of the coexistence of two different conformations of B-DTCP molecules in the open form. In one of them the two central CH_3 groups point in the same direction (C_s symmetry), in the other in opposite direction (C_2 symmetry). The central cyclopentene ring in principle breaks these symmetries, but it is useful to discuss the level structure and dynamics of B-DTCP in terms of the (approximate) symmetries C_s and C_2. Only the conformer with the C_2 symmetry can undergo the ring-closure reaction in a conrotatory fashion, according to the Woodward−Hoffmann rules.[11] In addition, the central methyl groups in the C_s symmetry cause substantial steric hindrance for the ring-closure reaction to occur. NMR data[19,20] on BTE compounds in solution indicate a close to 1:1 ratio between the C_2 and C_s forms. For most BTE-type switches, including the one studied here, interconversion between the two forms by rotation of the sidearms is a fast process on the NMR time scale at room temperature (milliseconds), but a slow process on the time scale of switching.[19,20] This means that in our experiments only about half of the molecules (those in the C_2 form) participate in the switching process.

To determine the quantum yield of ring closure, a 0.14 mM solution of B-DTCP in cyclohexane was irradiated by 300 μW UV light at a wavelength of 300 nm while the buildup of the lowest energy absorption band of the closed form was monitored with a weak probe at 550 nm. The known ratio between the number of B-DTCP molecules in open-ring and closed-ring forms allows us to calculate the extinction coefficient of the closed form $\epsilon_{\mathbf{1B},550} = (16.6 \pm 0.3) \times 10^3$ L mol^{-1} cm^{-1} and to convert the observed optical density into a number of absorbing molecules. The slope of the absorption curve, thus obtained, gives the value of 0.59 ± 0.1 switched molecule per absorbed photon (the error is mainly determined by the accuracy of the measurement of the power of the excitation light). By taking into account that there are two different conformations in the open-ring form of B-DTCP molecules at a close to 1:1 ratio[19,20] and only one conformer is able to switch, we can conclude that the quantum yield of ring closure in the case of switchable conformers is very close to 1.

During the time-resolved experiments on the ring-closure process, molecules in the open form are continuously being converted into the closed form. This means that finally both types of molecules will be excited by the pump pulses, which considerably complicates the interpretation of the observed transients. However, at low irradiation doses and not too small sample volume, the net effect of this buildup of photoproduct is limited and we can assume that only the forward reaction is probed. The average laser power in the pump−probe experiments is about 70 μW, which is equivalent to 1×10^{14} photons/s. With an optical density of 0.3 at the excitation wavelength and a switching probability of 0.59, this leads to the creation of $\sim 3 \times 10^{13}$ molecules in the closed form per second. Initially, the flow system contains a 30 mL solution of the molecules in the open form at a concentration of 0.7 mM, meaning that the total amount of optically active molecules is about 1.3×10^{19}. If we take as the acceptable limit for contamination of the solution the situation that at most 5% of the molecules are in the closed form, the sample can be irradiated for about 2.2×10^4 s (more than 6 h) before replacement is necessary.

In Figure 3, four typical transients are shown for excitation of the open form at 310 nm, and probing at the wavelengths cited in the figure. At all probe wavelengths, the dynamics can be separated into three regimes: First, ultrafast dynamics (0−0.5 ps) is observed over the whole 360−700 nm spectral region, then a 4.2 ps decay occurs with varying amplitude throughout the investigated spectral region, and finally some slower absorption changes occur on a few tens of picoseconds time scale. In the following sections, we will refer to these three regimes in the observed transients as preswitching dynamics, ring closure, and postswitching dynamics. The arguments for these assigments will be presented below and more extensively in the Theory and Discussion (section IV).

3.2. Preswitching Dynamics. The experimentally observed ultrafast part of the pump−probe response is summarized in the contour plot of Figure 4. In Figures 5 and 6 slices of this contour plot are shown along the frequency and time axes, yielding transient absorption spectra at particular delays and pump−probe transients at particular wavelengths, respectively. Following the spectra in time, a number of important observations can be made. The initial photoinduced absorption spectrum (at a pump−probe delay of 0 fs) is situated in the spectral region 430−480 nm. As shown in the top left frame of Figure 5, this

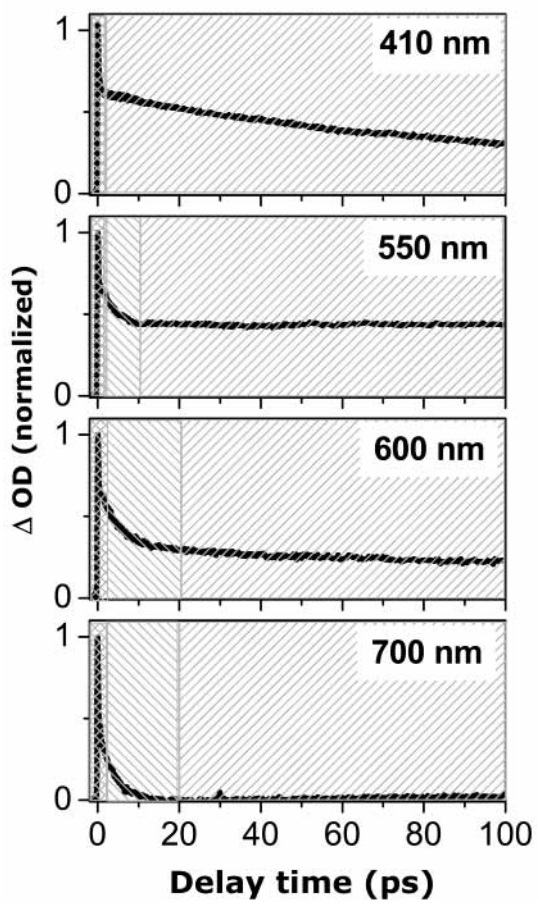

Figure 3. Normalized pump−probe transients for B-DTCP in cyclohexane at different probe wavelengths. Probe wavelengths are indicated in the panels. Areas corresponding to preswitching, switching and postswitching dynamics are marked by (xxx), (\\\), and (///), respectively.

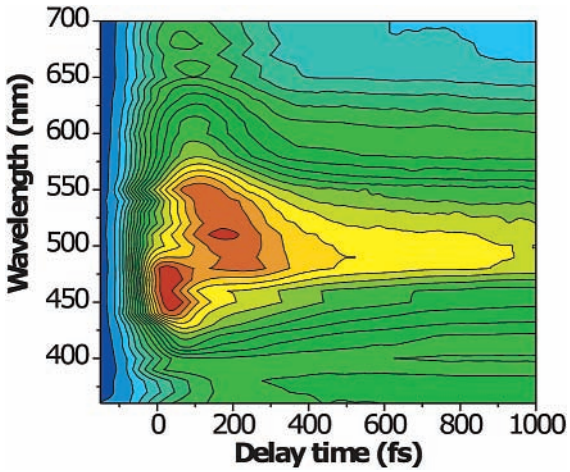

Figure 4. Contour plot representing the subpicosecond dynamics of B-DTCP in cyclohexane. The change in OD is plotted as a function of probe wavelength (vertical axis) for pump−probe delays up to 1 ps (horizontal axis).

spectrum closely resembles the photoinduced spectrum of the individual side groups of the switch, again confirming that the different parts of the molecule are only weakly coupled when the switch is in the open form. Similar observations were made by Tamai et al.[4] and Owrutsky et al.[6] in the cases of bithiophene- and bisthienylethene-based photochromic switches, respectively.

Whereas the photoinduced spectrum of the individual BT-chromophore side groups does not display any subpicosecond dynamics, the spectrum of the B-DTCP switch molecules rapidly changes. As the initially excited band rapidly decays, a red-shifted photoinduced absorption band in the 550−700 nm spectral region builds up on the same time scale. This precursor−successor relation is modified by a rapid blue spectral shift of the newly formed band from about 650 to 500 nm, during which also line broadening and a small drop in intensity occur. After a few hundred femtoseconds, no spectral changes occur anymore, as can, for instance, be seen from the right middle and bottom panels in Figure 5, where it is shown that the 500-fs and 2.5-ps transient spectra are practically identical. Only an overall decay of the spectrum on a picosecond time scale is observed, which, as we will argue below, is related to the process of ring closure.

To parametrize the dynamics, a simple phenomenological model was adopted, and the pump−probe transients, such as those displayed in Figure 6, were fitted globally. According to the model, the measured signal at a probe frequency ω during the first few picoseconds (when the postswitching dynamics can be neglected; see section 3.4) is expressed as

$$S_{SW}(\omega,t) = g_{pre}(\omega)e^{-k_{ps}t} + g_{suc}(\omega,t)(1 - e^{-k_{ps}t})e^{-k_{cl}t} + g_{cl}(\omega)(1 - e^{-k_{cl}t}) \quad (1)$$

Here, $g_{pre}(\omega)$ is the photoinduced absorption spectrum of the initially excited state (the precursor), $g_{suc}(\omega,t)$ is the photoinduced absorption spectrum of the state that appears with a small delay (the successor), and $g_{cl}(\omega)$ is the absorption spectrum of the closed form of the molecule that appears on a picosecond time scale (vide infra). The precursor goes over to the successor with rate constant k_{ps}, whereas the ring-closure rate constant is k_{cl}.

The spectra $g(\omega)$ can, in principle, be obtained from global fitting of the data. For the precursor and closed form of the molecule this is not difficult, because they dominate the spectrum at extremely short and long delay times, respectively. For the successor state the uncertainty is larger, although there are spectral regions (e.g., 550−700 nm) where the induced absorption is dominated by this state.

The spectrum $g_{suc}(\omega,t)$ is explicitly time dependent, due to the rapid blue shift and line broadening that is observed in Figures 4 and 5. Both effects were modeled in an exponential way, by writing for the central frequency $\omega_c = \omega_0 + \omega_{bl}(1 - \exp(-k_{bl}t))$ and for the line width $\Delta\omega = \Delta\omega_0 + \Delta\omega_{bl}(1 - \exp(-k_{bl}t))$. Here ω_{bl} and $\Delta\omega_{bl}$ are the amount of blue shift and the line broadening, respectively, and k_{bl} is the rate constant of both processes. A small drop in intensity of the signal was modeled with the same time constant k_{bl}. In the fitting procedure, the kinetic parameters were found to be $k_{ps}^{-1} = 70 \pm 15$ fs for the conversion from the initially excited state to the successor state, $k_{bl}^{-1} = 150 \pm 30$ fs for the spectral dynamics of the successor state, and $k_{cl}^{-1} = 4.2 \pm 0.6$ ps for the ring closure.

The model, just described, gives good results on the red side of the pump−probe spectrum, but yet another dynamical process has to be added to explain the transients to the blue of 500 nm. From 410 to 490 nm, a 325 fs decay component was observed, whereas from 350 to 380 nm a delayed growth of the signal with the same time scale occurs. This can be modeled by adding to eq 1 two more terms:

$$S_{NONSW}(\omega,t) = g_{pre}(\omega)e^{-k_{pnt}t} + g_{nsw}(\omega)(1 - e^{-k_{pnt}t}) \quad (2)$$

We believe this process to be totally unrelated to the switching from the open form to the closed form of the molecule. One reason for this conjecture is that in these wavelength regions

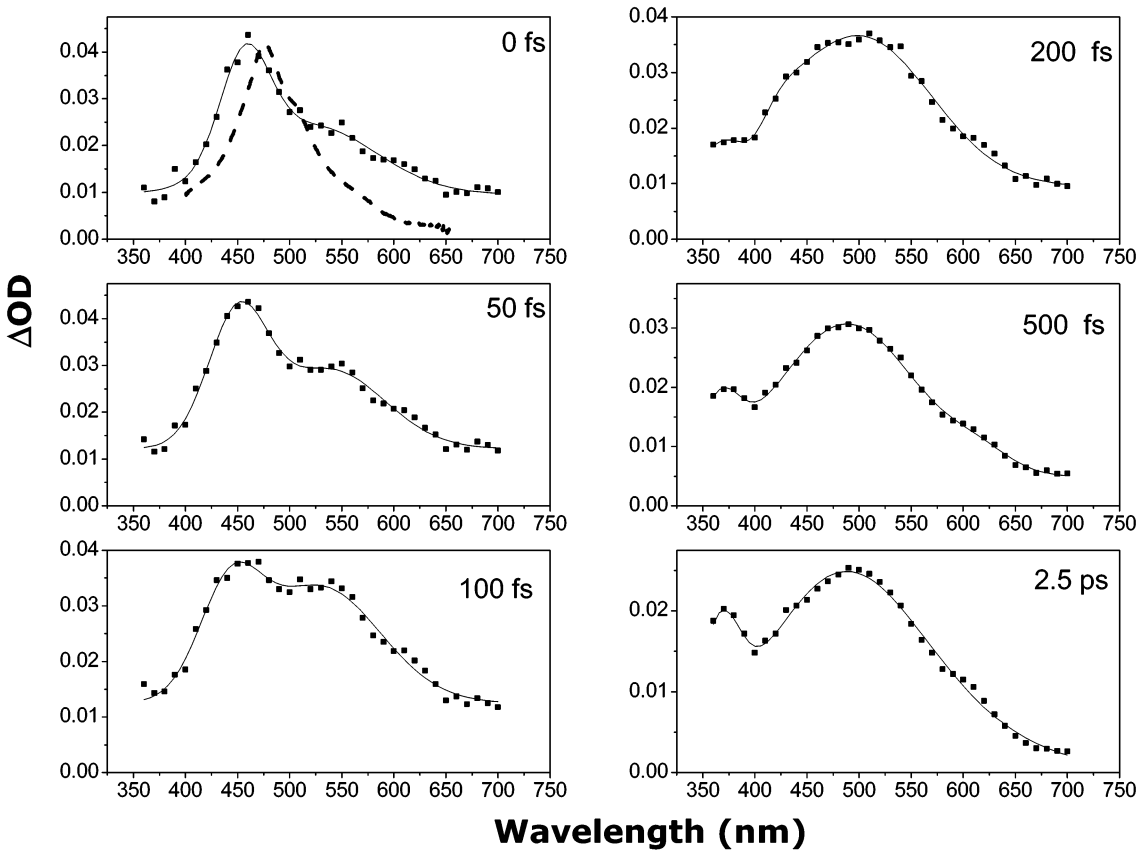

Figure 5. Transient absorption spectra of B-DTCP in cyclohexane at different delay times between pump and probe pulses. The delay times are indicated in the panels. The squares represent experimental data, and the solid lines are added as a guide for the eye. The dashed line in the upper left panel represents the transient absorption spectrum of the BT chromophore.

absorption bands appear that do not display any dynamics at the time scale of a few picoseconds. Therefore, the ring-closure rate constant k_{cl} does not appear in eq 2. This indicates that we are observing transient contributions from nonswitching conformers of B-DTCP. As discussed above, when the geometry of the side chains is such that the central CH_3 groups provide too much steric hindrance (C_s symmetry), ring closure does not occur.

In Figure 6, representative fitting curves are shown that reproduce all details of the dynamics and clearly demonstrate the success of the model. Both the processes of the switching molecules (eq 1) and those of the nonswitching molecules (eq 2) were included in the global fitting routine. Because the time scale of the ultrafast dynamics is very close to the time resolution of the experiments (for details see the experimental chapter), the response functions were deconvoluted from the experimental traces by using their cross-correlation function, as measured by sum frequency generation. The final result is as described above: both the switching and the nonswitching conformers display dynamics at ultrafast time scales ($k_{ps}^{-1} = 70$ fs and $k_{bl}^{-1} = 150$ fs for the switching ones and $k_{pn}^{-1} = 325$ fs for the nonswitching ones). However, on the time scale of a few picoseconds, only the switching conformers show further spectral changes. These are related to the ring-closure process ($k_{cl}^{-1} = 4.2$ ps).

3.3. Ring Closure. The ultrafast transients, reported above, are too fast to be associated with substantial movements of parts of the molecule. It is therefore unlikely that they reflect the time scale of the ring closure, which involves movements in both the central ring of the molecule and in the side chains. Instead, the time constant of $\tau_{cl} = 4.2$ ps that is present at all probe wavelengths, but with a varying amplitude, is a more likely candidate. The relative weight of this contribution to the observed transients as a function of frequency is displayed in Figure 7. It is clear that the dynamics occur predominantly from the successor state, defined above, whereas around 430 nm a band appears that relaxes much more slowly.

Similar time constants, in the range from 1 to 3 ps, were reported by Tamai,[4] Ern,[10] and Owrutsky[6] in the case of ring closure of dithienyl*perfluoro*cyclopentene derivatives. The main difference with these systems is the fluorination of the central cyclopentene bridge. The difference in time constants indicates that the fluorination speeds up the C−C bond formation. A detailed comparison between the dynamics of fluorinated and nonfluorinated switches will be published elsewhere.[21]

The absorption band at 430 nm, which does not display dynamics at a few picosecond time scale, suggests that there are species present that do not participate in the switching process. As discussed before, this is very likely due to molecules in the open-ring form with a conformation that prevents ring closure.[1,19,20] As discussed above, the photoexcitation of these molecules leads to rapid dynamics that is observable in the blue part of the pump−probe spectrum, until a state is reached that apparently has it absorption maximum at 430 nm.

At the probe wavelength of 700 nm, where only the successor state absorbs, the pump−probe signal relaxes to zero in a single-exponential way with the time constant of 4.2 ps. Therefore, it can be concluded that the switching efficiency of the conformers that are able to do so is very close to 1. This agrees with the overall value of the quantum yield of ring closure of 0.59 (see previous section), when the ground-state equilibrium ratio between the switching and nonswitching conformations of the open form of the B-DTCP molecules is about 3:2.

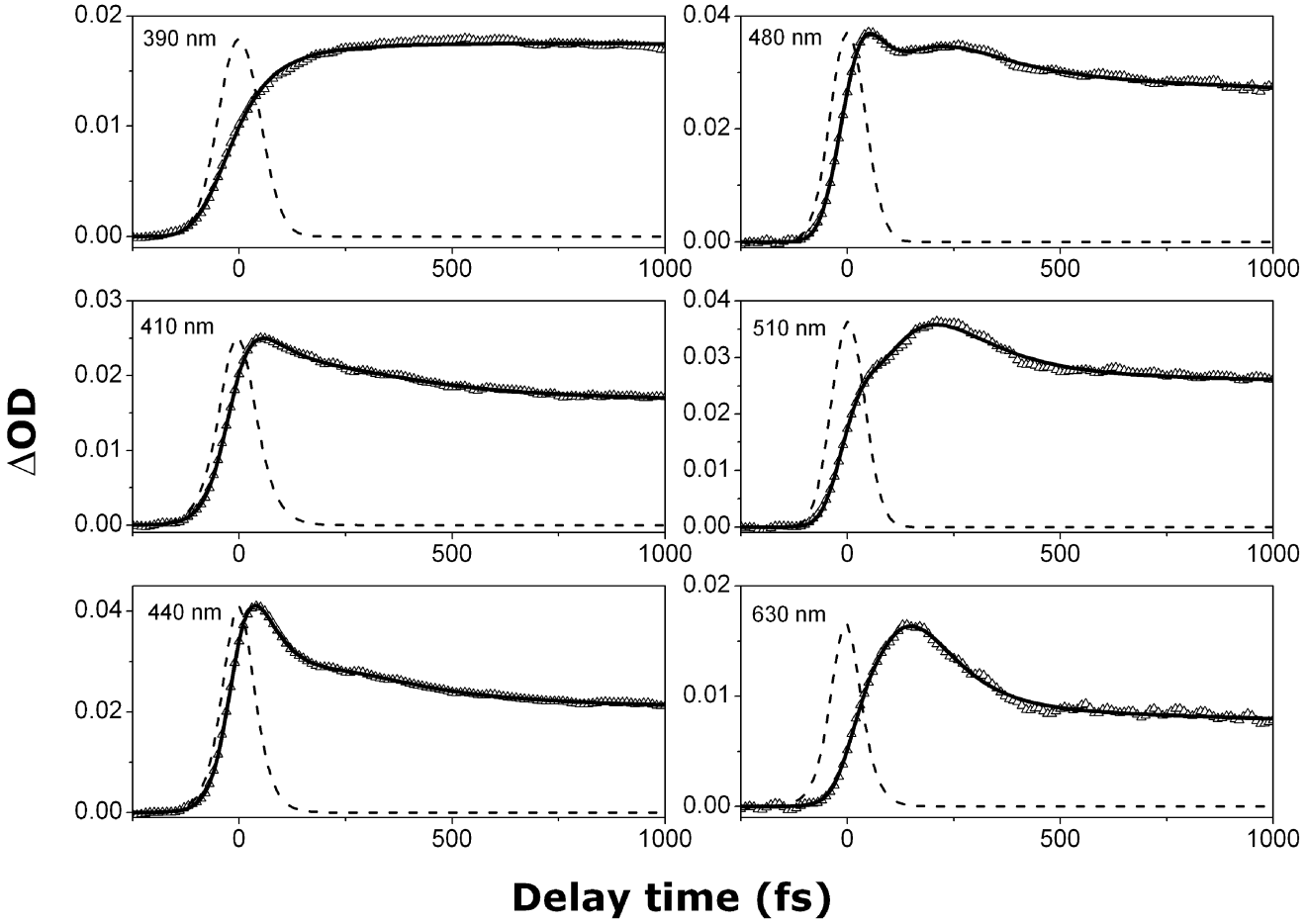

Figure 6. Pump−probe transients of B-DTCP in cyclohexane after excitation of the open form at 310 nm. The probe wavelength is shown in each panel. Dots represent experimental data, the solid lines are fits according to the model presented by eqs 1 and 2. An indication of the time resolution is given by dashed lines.

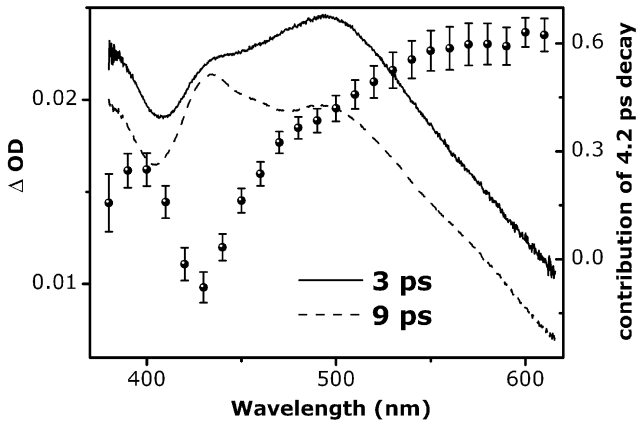

Figure 7. Transient spectra of B-DTCP recorded at delay times of 3 (solid line) and 9 (dashed line) ps. The circles with error bars show the relative contribution of the 4.2-ps decay process in the observed transients.

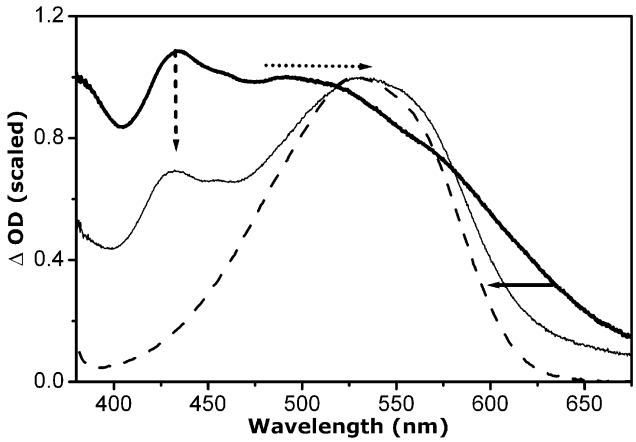

Figure 8. Transient spectra at a delay of 10 ps (bold line) and 100 ps (regular line). The spectra are normalized in the spectral region 500−550 nm. The dashed and dotted arrows indicate the decay of the band centered around 430 nm and the matching red shift of the band at 530 nm, respectively. The solid arrow points to the spectral narrowing as a result of vibrational cooling. The steady-state absorption spectrum of the closed form of B-DTCP (1B) (dashed line) is added for comparison.

3.4. Postswitching Dynamics. Figure 8 displays photoinduced absorption spectra in the time window 10−100 ps. To help visualize the spectral dynamics, the spectra are normalized in the region 500−550 nm. The main features are a decay of the absorption band at 430 nm, a narrowing on the red side of the spectrum (550−620 nm), and an apparent red shift of the band at about 520 nm. Although these effects are due to different phenomena, they occur on similar time scales. At the longest recorded pump probe delay of 100 ps, the shape of the photoinduced absorption spectrum begins to approach that of the ground-state absorption of the closed form.

The band, centered at 430 nm and attributed to the photoinduced absorption of the nonswitchable conformers, has partially decayed but is still clearly recognizable at a delay of 100 ps. This implies that the lifetime of the excited state of the

nonswitchable conformers is in the order of a few hundred picoseconds.

The narrowing on the red side of the spectrum is indicative of vibrational cooling, which apparently also is not completed, yet, at a delay of 100 ps. The switching process involves the radiationless transition of the successor state of the open form to the ground state of the closed form (see section IV). Consequently, there is a substantial amount of excess vibrational energy in the hot ground state of the closed form, directly after the switching. The decay constant, associated with the cooling process, is about 50 ps, when inferred from the data of Figure 8. This relatively low speed of cooling might originate from the large amount of vibrational energy that needs to be dissipated. In this case the cooling process becomes associated not only with the excitation of rotational modes of solvent molecules in the closest surrounding, but also with the distribution of the energy between the solvent molecules via translational motion.

Finally, the apparent shift of the maximum of the absorption band at 520 nm is due to the combination of both effects, just discussed. Both the decay of the 430 nm band of the nonswitchable conformers and the narrowing of the spectrum due to vibrational cooling of the hot ground state of the closed form molecules contribute to this effect.

3.5. Orientational Dynamics. More information about the ring-closure process and the pre- and postswitching behavior can be obtained from polarization sensitive measurements. In particular the dynamics of the photoinduced anisotropy can reflect changes in the orientation of the probed transition moments, for instance, due to conformational changes in the molecule when the switching takes place. The photoinduced anisotropy is defined as follows:

$$r(t) = \frac{\Delta OD_{||}(t) - \Delta OD_{\perp}(t)}{\Delta OD_{||}(t) + 2\Delta OD_{\perp}(t)} \quad (3)$$

Here, $\Delta OD_{||}(t)$ and $\Delta OD_{\perp}(t)$ are the optical density changes measured with parallel and orthogonal polarizations of the pump and probe beams, respectively. The time behavior of the photoinduced anisotropy $r(t)$ is not sensitive to the dynamics of population of the states during the dynamical processes but only traces the changes in the orientation of the transition dipole moment. In a liquid, where the molecules are randomly oriented and rapidly moving, the anisotropy can also be written as

$$r(t) = r(0)\frac{3\langle\cos^2\theta(t)\rangle - 1}{2} \quad (4)$$

In eq 4, $r(0)$ is the initially photoinduced anisotropy and $\theta(t)$ is the angle between the orientations of the transition dipole moments of the excitation at time $t = 0$ and of the probed transition at time t. When a single transition is probed in a sample of randomly oriented molecules, such as in isotropic solutions, the initial value of the photoinduced anisotropy $r(0)$ can range from $+0.4$ to -0.2, depending on whether the transition dipole moments involved in the excitation and probing are parallel ($+0.4$) or perpendicular (-0.2) in the molecular frame. When more than one transition is probed (or excited), a summation over all possible combinations of transitions is needed for evaluation of the total anisotropy.

The photoinduced anisotropy relaxes to zero both through electronic and nuclear rearrangements that alter the direction of the transition dipole moment, as well as through rotational diffusion.[22−24] In Figure 9 it is shown that the anisotropy of

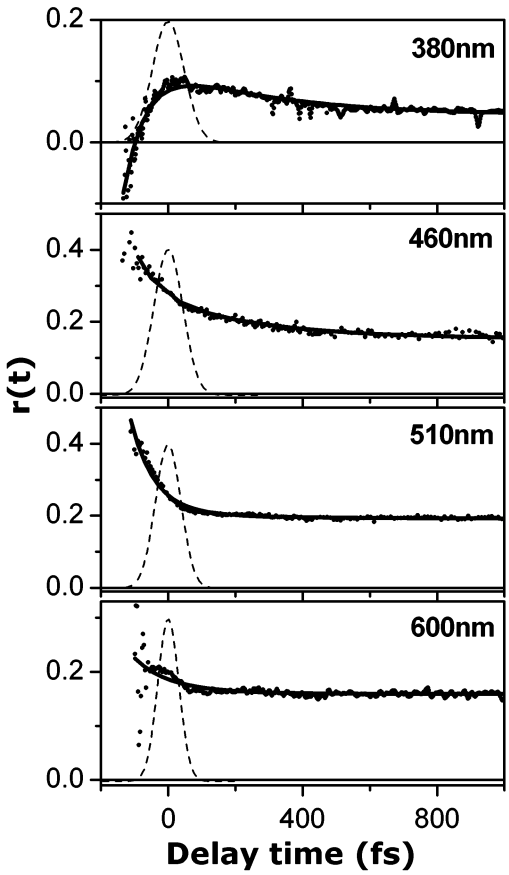

Figure 9. Early-time dynamics of the photoinduced anisotropy at different probe wavelengths (indicated in the panels). Dots represent experimental data; the solid lines are two-exponential fits with time constants of 70 and 325 fs. An indication of the time resolution in each case is given by the dashed lines.

B-DTCP displays ultrafast dynamics over the entire probe spectrum. Determination of the initial value of the photoinduced anisotropy is difficult because of the limited time resolution of these experiments and also because of possible coherent coupling effects that may take place during the first tens of femtoseconds, within the dephasing times of the optical transitions involved.[25] Nevertheless, it is clear that in the spectral region 460−510 nm the initial value of the photoinduced anisotropy is positive and close to the theoretical maximum of 0.4, whereas on the blue side it is negative and possibly close to its theoretical minimum of -0.2. Apparently, two optical transitions are probed that are polarized perpendicular to each other.

The kinetic parameters, found for the orientational dynamics on femtosecond time scales, agree with those of the pump−probe transients discussed above. To the red of 500 nm only a 70 fs component is present, whereas to the blue both 70 and 325 fs transients are observed. The fits support the notion that these time constants are related to the kinetics of two different species.

In Figure 10, the photoinduced anisotropy is followed on a picosecond time scale. Over most of the spectral range the anisotropy rises exponentially with a time constant of 8 ps, before relaxing via rotational diffusion with a time constant of about 100 ps. In the upper left panel it is shown that around 410 nm, where no switching dynamics was observed in the case of the pump−probe experiments (see Figure 7), the dynamical process with time constant 8 ps is absent. This indicates that

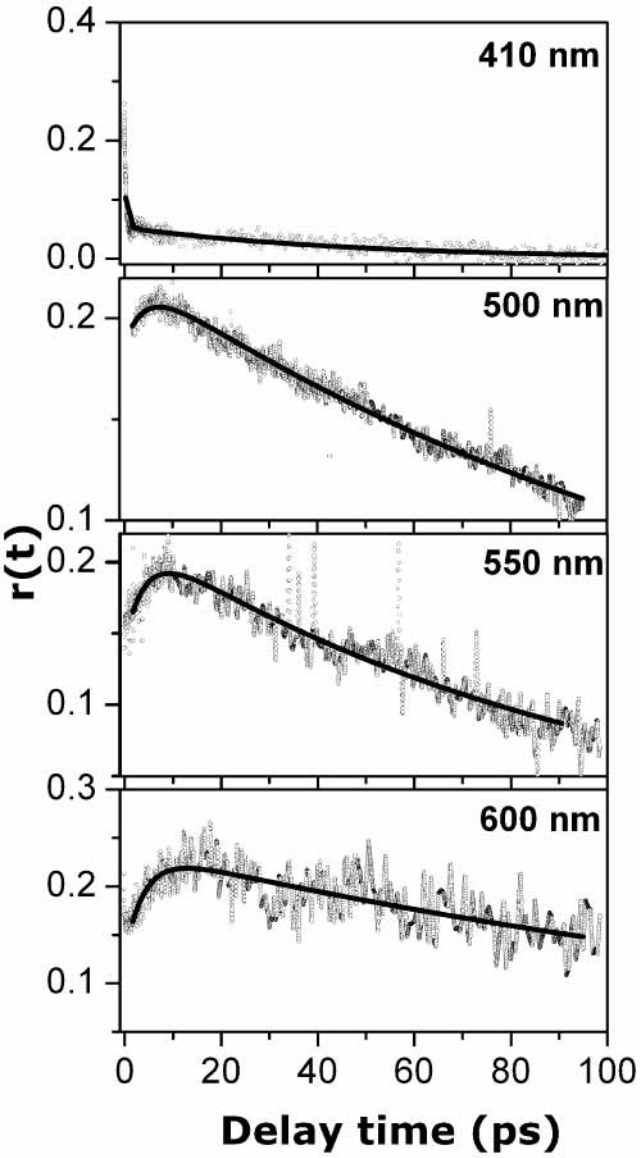

Figure 10. Transients of the photoinduced anisotropy, recorded at different probe wavelengths in the time interval 0−100 ps (probe wavelengths are indicated in the panels). Experimental results are given by the points; the solid lines are two-exponential fits with time constants of 8 and 100 ps.

the 8 ps rise at the other wavelengths is related to the ring closure.

We tentatively attribute the 8 ps component in the transients of the photoinduced anisotropy to the motion of the thienyl wings of the B-DTCP molecule toward coplanarity as a result of the ring closure. The lower limit for the time constant of this "forced" movement towards coplanarity is of course the switching time itself, i.e., 4.2 ps. However, due to the moment of inertia of these thienyl side groups, some larger time constant may be expected. An indication for the size of this effect may be obtained from the reorientation times of the individual BT chromophores, which we measured to be $\tau_{or1} = 2$ ps and $\tau_{or2} = 18$ ps. The combination of torque induced by the ring closure and moment of inertia of the side groups may very well lead to the observed value of 8 ps in the orientational dynamics.

IV. Theory and Discussion

The experimental results of the previous section indicate that the switching dynamics of B-DTCP is quite complicated, when studied in detail. Very fast femtosecond kinetics, including rapid rotations of transition moments, is followed by picosecond ring closure, which, in turn, leads to inertial forced conformational dynamics and vibrational cooling on much longer time scales. The femtosecond processes are so fast that nuclear displacements during that time can only occur over a very limited excursion range. In particular, the very fast changes in the induced anisotropy indicate that transitions between electronic states are involved, rather than movements of part of the molecule.

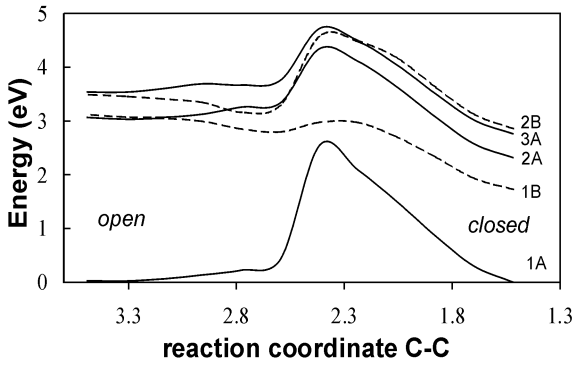

Figure 11. Potential energy curves for the lowest electronic energy levels, calculated for the B-DTCP molecule in C_2 symmetry. A and B denote the two possible different symmetries. For a definition of the reaction coordinate see text.

To interpret these experimental findings, we calculated the geometries, energy levels, and excitation spectra using density functional theory and time-dependent density functional theory. For this purpose, the Amsterdam Density Functional Program Package (ADF)[26−28] was used, which is able to provide accurate solutions of the Kohn−Sham (KS) equations even for fairly large systems. For the ground-state calculations we used the local density approximation, based on the parametrization of the electron gas data given by Vosko, Wilk, and Nusair.[29] The basis sets used were of triple ζ plus polarization Slater type function (STO) quality (basis IV in ADF).

Excited states were calculated using time-dependent density functional theory (TDDFT), as implemented in the RESPONSE part of ADF. Because TDDFT describes (in principle, exactly) how the electron density changes in time under the influence of a time-dependent perturbation, and because this time-dependent density will resonate at the excitation energies of the system, linear response theory based on TDDFT is able to provide both these excitation energies as well as the corresponding oscillator strengths. As discussed before, we will use the nomenclature of C_2 symmetry for the switching conformer where the central CH_3 groups point in opposite directions, and C_s symmetry is assumed for the nonswitching conformers with the central CH_3 groups pointing toward each other.

In Figure 11, the lowest electronic energy levels are depicted as a function of a reaction coordinate. The reaction coordinate is defined as the distance between the two C atoms in the central ring, which become bonded in the closed form. All other coordinates are optimized for the lowest ground-state energy at each position along this reaction coordinate. Note that this path conserves the original C_2 symmetry. Clearly, a high barrier separates the open and closed form in the ground state, which explains why both are thermally stable and can only be switched into each other by excited-state pathways.

In the open form of the molecule, the low-lying electronically excited states come in almost degenerate pairs, each containing one state of the two possible symmetries A and B. The first two excited states arise from charge transfer like excitations

from the central bond HOMO π-orbital to the LUMO's on the chromophore side chains. Because the two chromophore π-systems have very little interaction in the open form (they are almost orthogonal to each other), the two chromophore LUMO's combine to one orbital of *a* symmetry and one orbital of *b* symmetry, leading to the two nearly degenerate excited states 2A and 1B. Both transitions from the ground state have very low oscillator strengths, because the HOMO and the LUMO's are located in different parts of the molecule. Note that the corresponding transition is, of course, absent in the isolated chromophores, because the central bond is then not present.

The second pair of excited states are of an entirely different character. They turn out to correspond to the HOMO−LUMO transitions in the chromophores themselves. Again, both transitions combine to A and B states that are almost degenerate, due to the small interaction between the chromophore π-systems. In this case we calculate the 2B state to have considerable oscillator strength, whereas the 3A state is essentially dark. This is easily understood when one realizes that 2B corresponds to an excited state that has the approximate form $|L \rightarrow L^*\rangle + |R \rightarrow R^*\rangle$, where L and L* are the left chromophore HOMO and LUMO orbitals and R and R* are the corresponding orbitals on the right side of the molecule. For this state, the monomer transition dipole moments interfere constructively, leading to large oscillator strength, whereas for the 3A state with character $|L \rightarrow L^*\rangle - |R \rightarrow R^*\rangle$, the monomer transition moments interfere destructively. The lowest energy optically allowed excitation of the open form of B-DTCP therefore is the 1A → 2B transition. Due to the weak coupling between the left and right part of the molecule, this transition closely resembles the first excitation of the isolated chromophores. The pump−probe spectrum at zero delay therefore is essentially the same as in the isolated chromophores, in accordance with the experimental findings above (see Figure 5).

The rapid fluctuations in the immediate environment of the switch lead to symmetry breaking and therefore coupling of the A and B states. Hence, the originally excited 2B state relaxes to a thermal equilibrium with the almost degenerate 3A state. The important point is that this relaxation process does not involve any change of geometry of the switch and therefore it can be expected to proceed extremely rapidly. We therefore identify it with the fastest time experimentally observed, i.e., the 70 fs precursor−successor sequence. The 150 fs spectral dynamics that follows is due to motion on the new potential energy surface. The change of character from 2B to 3A is experimentally confirmed not only by the rapid changes in the pump−probe spectra, but also by the fast loss of anisotropy, which is indicative of a rapid change in the direction of the probed dipole moment.

For the nonswitching molecules a similar coupling scheme holds. Due to the different geometry, the relative position of the 2B and 3A states is somewhat different and also the coupling between these two states might be slightly modified. As a result, the decay occurs with a time constant of 325 fs, instead of 70 fs. This was observed both in the pump−probe and the transient anisotropy measurements. The major difference occurs at later times, however. Where one conformer displays ring closure, the other cannot perform this process due to steric hindrance of the two central CH_3 groups, which prevent the relevant C atoms from approaching each other close enough.

According to Figure 11, both the 2B and 3A states of the switching molecules exhibit a high barrier along the reaction path. However, there is a lower lying state, 1B, that does not contain the same barrier. It is therefore this state that gives rise to the actual ring closure. As we will argue now, it is the relaxation of the 2B/3A states to the 1B state that is the rate determining step in going from the open to the closed form. From Figure 11, it is clear how relaxation may occur: the 2B and 2A states cross a little way along the reaction coordinate. When the C_2 symmetry is broken, the crossing will in fact be avoided. This means that there will be a conical intersection between the two surfaces, leading to a feasible relaxation mechanism.[30] We believe that this process gives rise to the 4.2 ps transients, observed in the pump−probe data. The subsequent mixing of the near degenerate states 2A and 1B is supposed to be a fast process again, and also the downhill motion from the open to the closed form in the state 1B will be very rapid. This model is supported by the fact that the anisotropy in the wavelength range 460−700 nm after a femtosecond decay recovers again on a picosecond time scale: a B state is populated again.

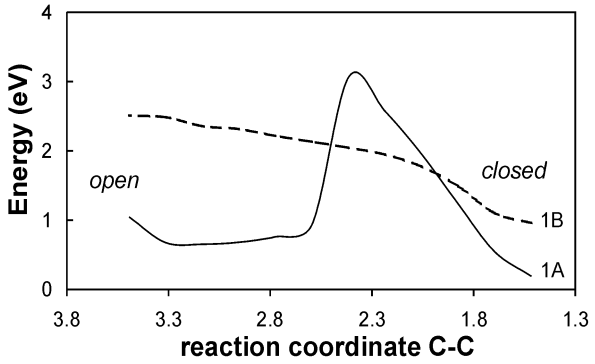

Figure 12. Potential energy curves for the 1A and 1B electronic states, but optimized for the 1B excited state instead of the ground state (as in Figure 11).

The final step in the switching process, i.e., the motion along the 1B potential to the closed form, is actually not depicted correctly in Figure 11. The energy levels are plotted along the minimum energy reaction path in the ground state, which is not the minimum (electronic) energy path in the 1B excited state. For the excited-state minimum energy path, the calculations give the potential energy curves shown in Figure 12. The energy barrier in the ground state has of course increased, whereas the 1B excited state has come down in energy. Because the motion along the reaction coordinate is rather fast, it is possible that the system in the 1B state does not have enough time to find its minimum energy configuration everywhere along this curve. In that case the potential energy surface will be somewhat different.

The fact that the two states in Figure 12 cross at two points means that at slightly deformed nonsymmetric geometries there will be avoided crossings; hence two conical intersections appear. These conical intersections provide a mechanism for the relaxation of the excited 1B state to the 1A ground state and, though the left crossing in the graph would lead back to the original open form ground state, the right crossing point leads to the ground state of the closed switch, thus completing the switching process. The large angle of the two potential energy curves at the first crossing point explains why hardly any back-transfer to the ground state of the open form occurs.[31,32]

V. Summary and Conclusions

The switching behavior of B-DTCP, which is based on ring closing, was studied in detail with femtosecond nonlinear optical

experiments and density functional calculations. The overall dynamics can be separated into preswitching dynamics, the ring closure proper, and postswitching dynamics. After optical excitation, the system propagates through a rather complicated sequence of electronical states. The coupling between these states, governed by geometrical distortions, determines the reaction rate of the overall process. After the ring closure, forced geometrical changes and vibrational cooling determine the dynamics of the optical response.

The overall picture of the ring-closure reaction is as follows: first, the initially excited state rapidly, with a time constant of 70 fs, equilibrates with an electronic state of different symmetry (in terms of the energy levels of Figure 11: $1A + h\nu \rightarrow 2B \leftrightarrow 3A$). Second, population relaxation takes place with a time constant of 4.2 ps, to a state that experiences energy lowering when ring closure occurs ($2B \rightarrow 2A \rightarrow 1B$). Third, the formation of the central C−C bond induces rotation of the side groups of the molecule to a nearly coplanar conformation, with a time constant of 8 ps ($1B \rightarrow 1A^*$). Fourth, the vibrationally hot ground state of the closed conformer relaxes to thermal equilibrium with a time constant of about 50 ps ($1A^* \rightarrow 1A$). This completes the switching process.

The combination of time-resolved optical experiments with theoretical analysis of the electronic structure allows us to obtain this detailed picture of both the population and the conformational dynamics of the switching process. We expect that the insight, thus obtained, will provide important clues for the design of new switches with characteristics that can be predicted from the theory with a fair level of confidence.

Acknowledgment. This work was supported by the "Nederlandse Organisatie voor Wetenschappelijk onderzoek" (NWO). R.T. is grateful for the support by EU FULPROP PROGRAM "FMRX-CT97-0155". The Royal Netherlands Academy of Sciences is gratefully acknowledged for a fellowship for J.v.E..

References and Notes

(1) Irie, M. *Chem. Rev.* **2000**, *100*, 1685.
(2) Tamai, N.; Miyasaka, H. *Chem. Rev.* **2000**, *100*, 1875.
(3) Miyasaka, H.; Araki, S.; Tabata, A.; Nobuto, T.; Mataga, N.; Irie, M. *Chem. Phys. Lett.* **1994**, *230*, 249.
(4) Tamai, N.; Saika, T.; Shimidzu, T.; Irie, M. *J. Phys. Chem.* **1996**, *100*, 4689.
(5) Ohtaka, N.; Hase, Y.; Uchida, K.; Irie, M.; Tamai, N. *Mol. Cryst. Liq. Cryst.* **2000**, *344*, 83.
(6) Owrutsky, J. C.; Nelson, H. H.; Baronavski, A. P.; Kim, O.-K.; Tsivgoulis, G. M.; Gilat, S. L.; Lehn, J.-M. *Chem. Phys. Lett.* **1998**, *293*, 555.
(7) Ern, J.; Bens, A. T.; Bock, A.; Martin, H.-D.; Kryschi, C. *J. Lumin.* **1998**, *76&77*, 90.
(8) Ern, J.; Bens, A. T.; Martin, H.-D.; Mukamel, S.; Schmid, D.; Tretiak, S.; Tsiper, E.; Kryschi, C. *Chem. Phys.* **1999**, *246*, 115.
(9) Miyasaka, H.; Murakami, M.; Itaya, A.; Guillaumont, D.; Nakamura, S.; Irie, M. *J. Am. Chem. Soc.* **2001**, *123*, 753.
(10) Ern, J.; Bens, A.; Martin, H.-D.; Mukamel, S.; Schmid, D.; Tretiak, S.; Tsiper, E.; Kryschi, C. *J. Lumin.* **2000**, *87−89*, 742.
(11) Woodward, R. B.; Hoffman, R. *The conservation of orbital symmetry*; Verlag Chemie/Academic Press: Weinheim, 1970.
(12) Nakamura, S.; Irie, M. *J. Org. Chem.* **1988**, *53*, 6136.
(13) Ern, J.; Bens, A. T.; Martin, H.-D.; Mukamel, S.; Tretiak, S.; Tsyganenko, K.; Kuldova, K.; Trommsdorff, H. P.; Kryschi, C. *J. Phys. Chem. A* **2001**, *105*, 1741.
(14) Bens, A. T.; Ern, J.; Kuldova, K.; Trommsdorff, H. P.; Kryschi, C. *J. Lumin.* **2001**, *94−95*, 51.
(15) Lucas, L. N.; Esch, J. v.; Feringa, B. L.; Kellogg, R. M. *Chem. Commun.* **1998**, 2313.
(16) Tsivgoulis, G. M.; Lehn, J.-M. *Chem. Eur. J.* **1996**, *2*, 1399.
(17) Wilhelm, T.; Piel, J.; Riedle, E. *Opt. Lett.* **1997**, *22*, 1494.
(18) Reuther, A.; Laubereau, A.; Nikogosyan. *Opt. Commun.* **1997**, *141*, 180.
(19) Uchida, K.; Nakayama, Y.; Irie, M. *Bull. Chem. Soc. Jpn.* **1990**, *63*, 1311.
(20) Irie, M.; Sakemura, K.; Okinaka, M.; Uchida, K. *J. Org. Chem.* **1995**, *60*, 8305.
(21) Hania, P. R.; Lucas, L. N.; Pugzlys, A.; Esch, J. v.; Feringa, B. L.; Duppen, K. To be published.
(22) Lakowicz, J. R. *Principles of fluorescence spectroscopy*, 2nd ed.; Kluwer Academic/Plenum Publishers: New York, 1999.
(23) Fleming, G. R. *Chemical applications of ultrafast spectroscopy*; Oxford University Press: New York, 1986; Vol. 13.
(24) Waldeck, D.; Jr., A. J. C.; McDonald, D. B.; Fleming, G. R. *J. Chem. Phys.* **1981**, *74*, 3381.
(25) Wynne, K.; Hochstrasser, R. M. *Chem. Phys.* **1993**, *171*, 179.
(26) Baerends, E. J.; Ellis, D. E.; Ros, P. *Chem. Phys.* **1973**, *2*, 41.
(27) Guerra, C. F.; Visser, O.; Snijders, J. G.; Velde, G. t.; Baerends, E. J. *Methods and Techniques in Computational Chemistry*; STEF: Cagliari, Italy, 1995.
(28) Velde, G. t.; Baerends, E. J. *J. Comput. Phys.* **1992**, *99*, 84.
(29) Vosko, S. H.; Wilk, L.; Nusair, M. *Can. J. Phys.* **1980**, *58*, 1200.
(30) Turro, N. J. *Modern molecular photochemistry*; University Science Books: Mill Valley, CA, 1991.
(31) Landau, L. *Phys. Z. USSR* **1932**, *46*, 2.
(32) Zener, C. *Proc. R. Soc. London A* **1932**, *137*, 696.